Supplementary Figure Legends

Figure S1: Quality controls of the ^{89}Zr-Df- aTCRmu-F(ab')$_2$ production

(A) SDS-PAGE gel of the aTCRmu-F(ab')$_2$ fragment after pepsin digestion. The following samples are shown: lane 1: the protein marker, lane 2: aTCRmu-F(ab')$_2$ under non-reducing conditions and lane 3 aTCRmu-F(ab')$_2$ fragments under reducing condition. (B) UV-profiles in SE-HPLC are depicted of the full aTCRmu antibody (upper graph) and the digested F(ab')$_2$ fragment (lower graph). UV signals are shown as mAU. (C) Profile of the ^{89}Zr-labeled Df-aTCRmu-F(ab')$_2$ analyzed by radio-ITLC. Radioactive signal is provided as counts/seconds (γ). (D) Representative autoradiographs of SDS-PAGE gels of liver, blood and kidney homogenates of NSG mice injected with ^{89}Zr-Df-aTCRmu-F(ab')$_2$ and sacrificed 6 h, 24 h and 48 h post injection (n=3). Intact ^{89}Zr-Df-aTCRmu-F(ab')$_2$ is presented in the reference lane and areas of probe traces are indicated by the white dashed line. ROIs were placed on the level of intact tracer and signal intensities were calculated.

Figure S2: *In vitro* labeling of TCR2.5D6 iRFP T_{CM} by ^{89}Zr-Df- aTCRmu-F(ab')$_2$

(A) Flow cytometry anti-TCRmu staining of TCR2.5D6 iRFP T_{CM} labeled before by ^{89}Zr-Df-aTCRmu-F(ab')$_2$ (solid line) and non-labeled TCR2.5D6 iRFP T_{CM} (dotted line). Isotype control on TCR2.5D6 iRFP T_{CM} (dashed line). (B) Counts per minute (CPM) of different numbers of ^{89}Zr-Df-aTCRmu-F(ab')$_2$ labeled TCR2.5D6 iRFP T_{CM} (n=3) and non-transduced T_{CM} pellets (n=2) used for the "*in vivo* spot assay" before s.c. injection and PET/CT imaging. cpm are shown as mean ± SD.

Figure S3: Experimental setting and *ex vivo* analyses of intra-tumoral quantified TCR2.5D6 iRFP T_{CM} after adoptive transfer and imaging *in vivo*

(A) Schematic overview of the experimental setting. NSG mice were injected s.c. with $1x10^7$ ML2-B7 cells into the right and $1x10^7$ ML2-B15 cells into the left flank followed by 1Gy total body irradiation (TBI). Eight days after tumor inoculation, defined numbers of TCR2.5D6 iRFP T_{CM} or non-transduced T_{CM} were adoptively transferred intravenously and irradiated (80Gy) hIL -15 producing NSO-cells were injected i.p. at the same day. Three days after T_{CM} injection, ^{89}Zr-Df-aTCRmu-F(ab')$_2$ was injected intravenously and PET/CT imaging was performed after 48 h. (B) *Ex vivo* biodistribution analysis of ^{89}Zr-Df-aTCRmu-F(ab')$_2$ in indicated organs 48 h post injection. Mean ± SD of %ID/g are depicted for the animal groups (n=2 for group I and IV, n=3 for group II and III) and n=2 treated with non-transduced T_{CM}. (C) Quantitative evaluation of tumors-to-muscle ratios 48 h post ^{89}Zr-Df-aTCRmu-F(ab')$_2$ injection. Mean ± SD of the ratios are depicted for the animal groups (n=2 for group I and IV, n=3 for group II and III) and n=2 treated with non-transduced T_{CM}. Dashed line indicates maximum background ratio in the groups. (B-C) Representative data of one out of four experiments is shown. (D) *Ex vivo* flow cytometry analysis of ML2-B7 and ML2-B15 tumors. hCD5/hCD45 positive populations representing engrafted T_{CM} (upper panel). iRFP positive TCR2.5D6 $T_{CM,}$ out of hCD5/hCD45 positive populations used for quantification of the absolute number of TCR2.5D6 iRFP T_{CM} (lower panel).

Figure S4: Relation of *ex vivo* quantified TCR2.5D6 iRFP T_{CM} after adoptive T-cell transfer *in vivo* and image-based probe accumulation

(A-C) Relation of detected absolute numbers of TCR2.5D6 iRFP T_{CM} to mean activity at ML2-B7 tumors in three individual experiments injected with $3.0x10^6$, $0.6x10^6$ and $0.3x10^6$ TCR2.5D6

iRFP T_{CM} is shown. Total number of TCR2.5D6 iRFP T_{CM} and image-based mean activity [Bq/ml] are shown.

Figure S5: Correlation of number of tumor infiltrated TCR2.5D6 iRFP T_{CM} and probe accumulation

Linear regression analysis of number of detected TCR2.5D6 iRFP T_{CM} in ML2-B7 tumors and corresponding %ID/g of the biodistribution (A) and image-based activity (Bq/ml) (B) derived from four different experiments (n=43).

Supplementary Figure S1

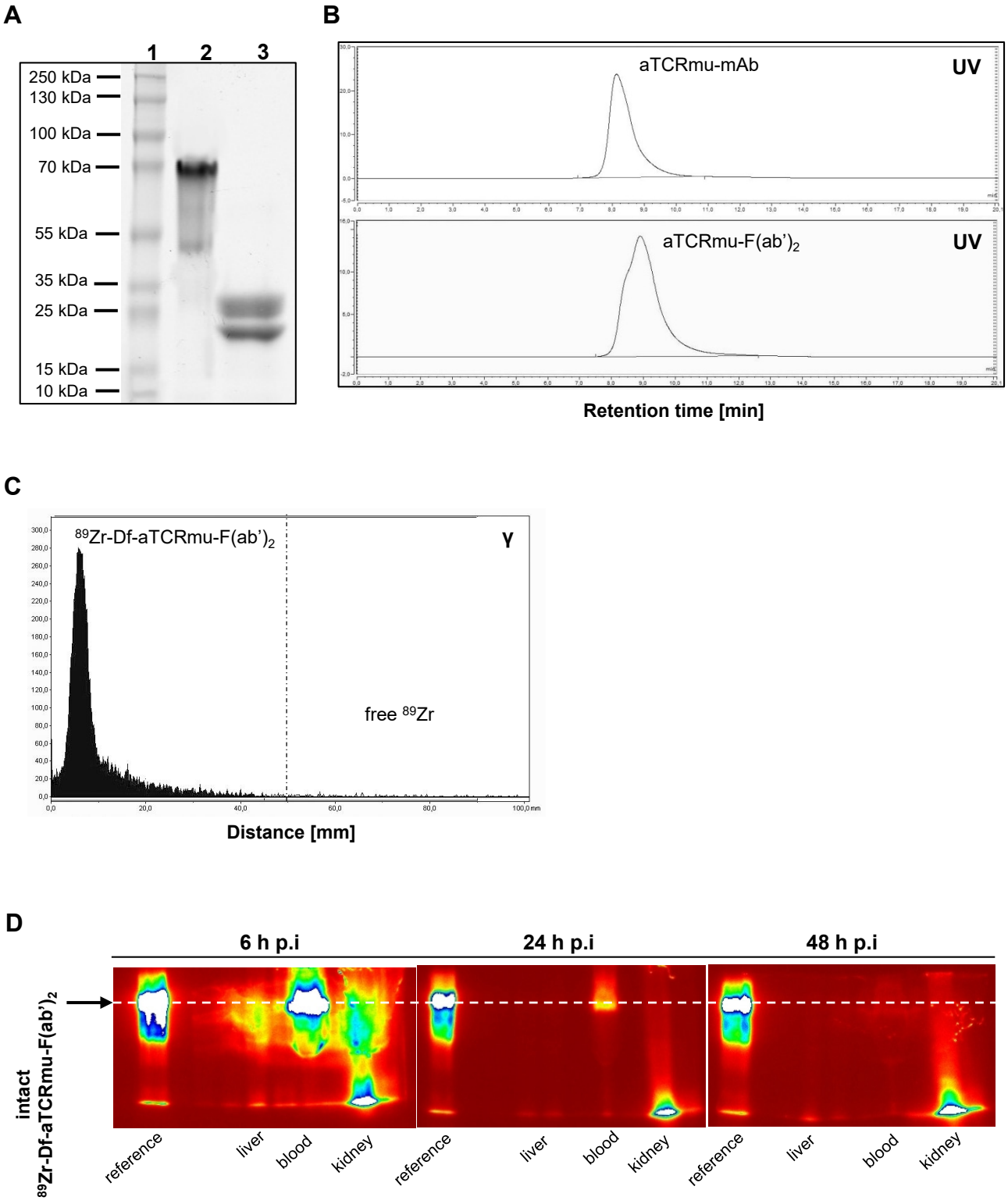

Supplementary Figure S2

A

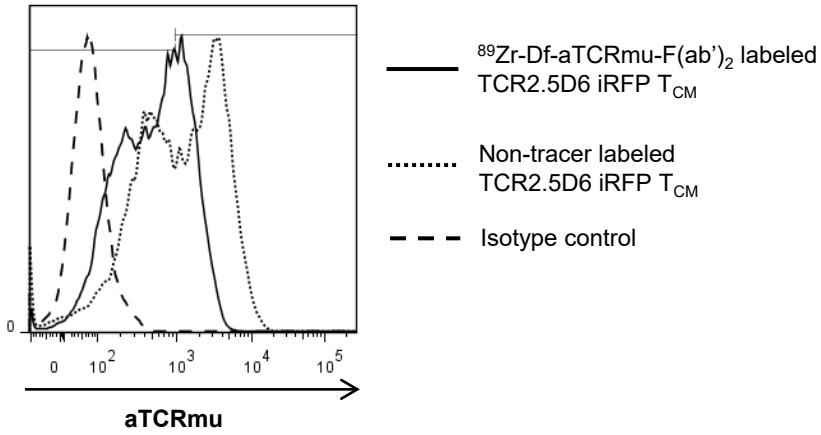

B

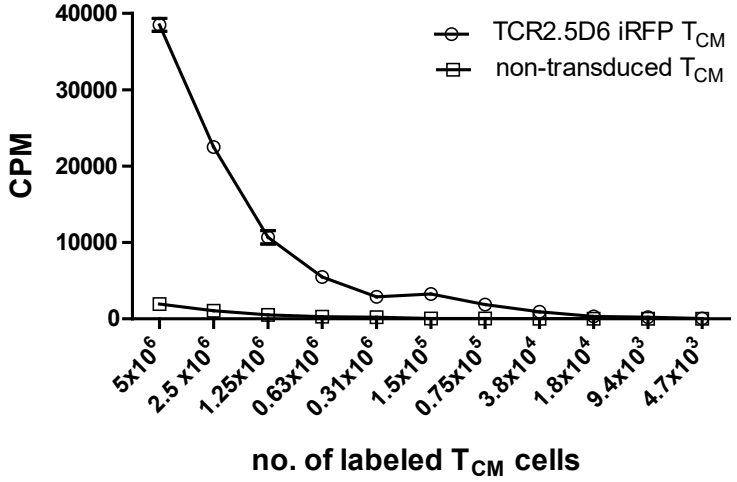

Supplementary Figure S3

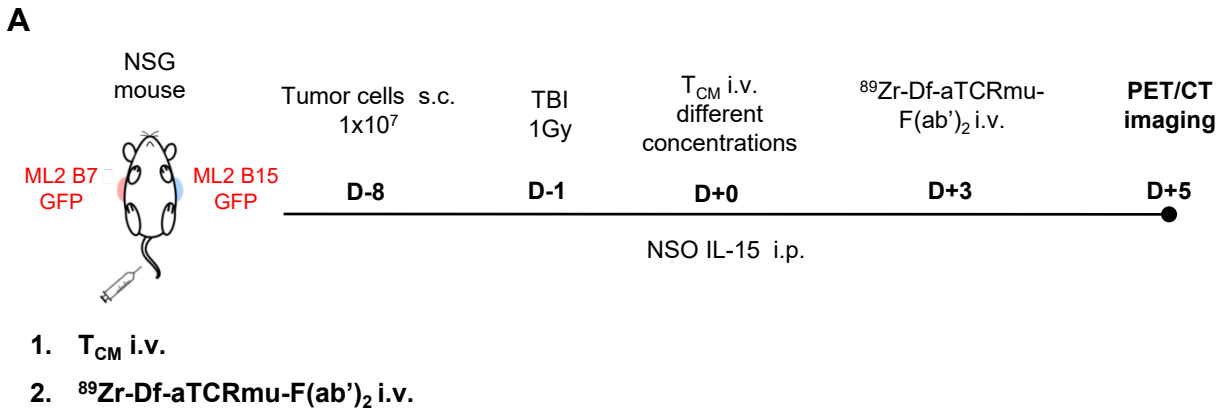

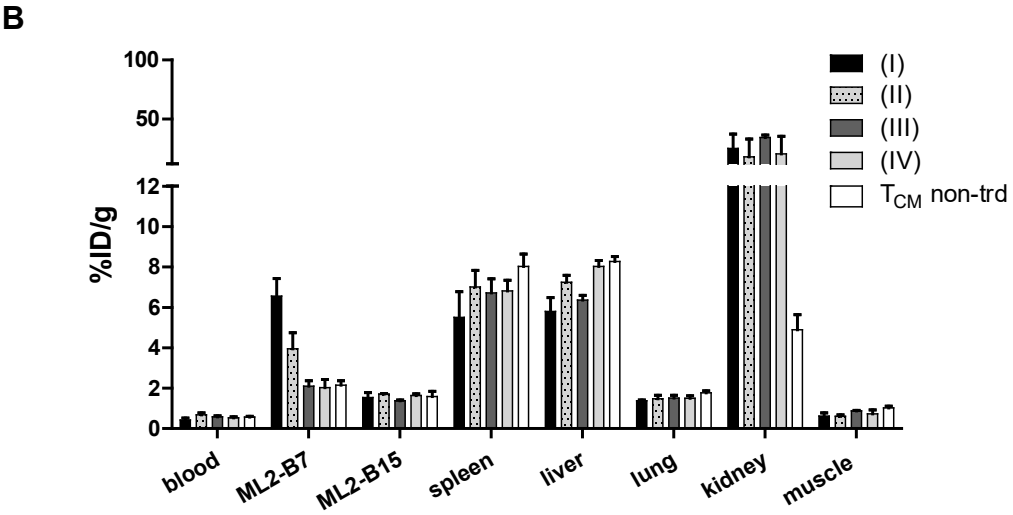

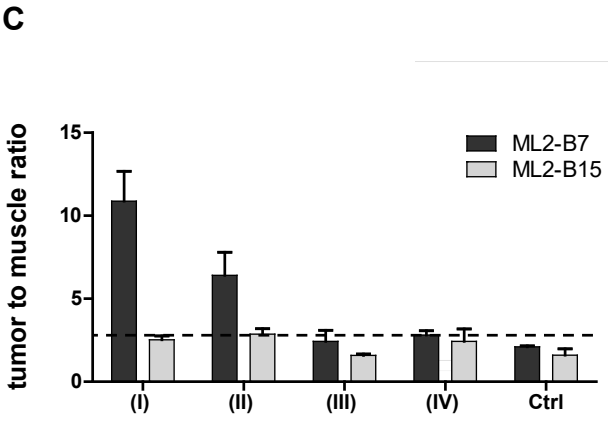

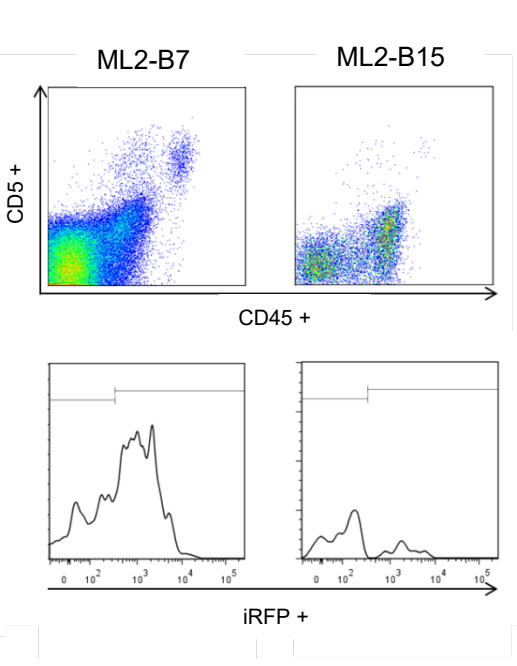

Supplementary Figure S4

A

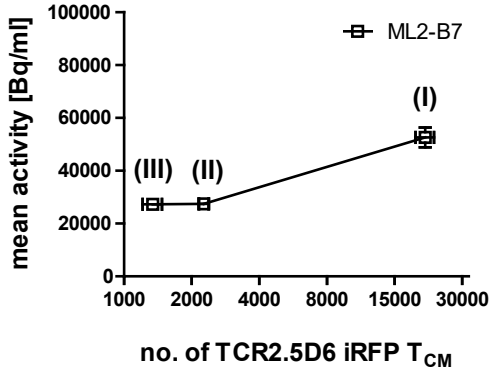

B

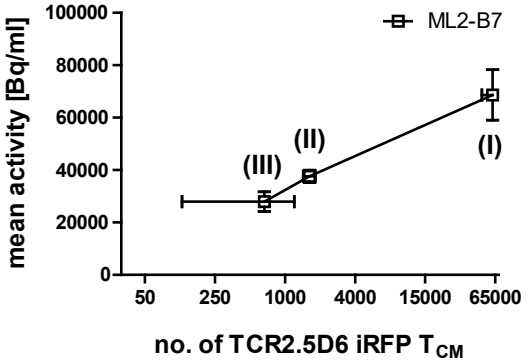

C

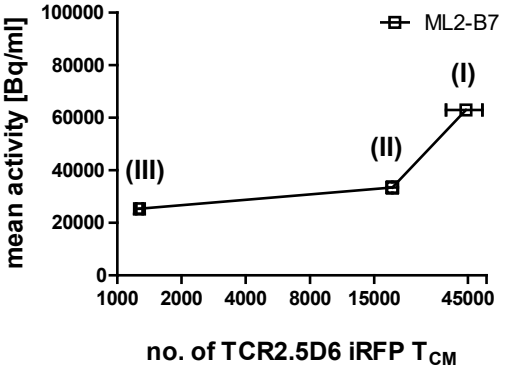

Supplementary Figure S5

A

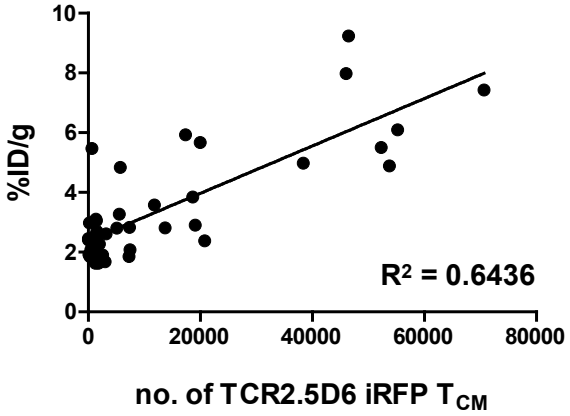

B